Applied Physics Letters

Transparent p-type SnO_x thin film transistors produced by reactive rf magnetron sputtering followed by low temperature annealing

Cite as: Appl. Phys. Lett. **97**, 052105 (2010); https://doi.org/10.1063/1.3469939
Submitted: 09 February 2010 . Accepted: 07 July 2010 . Published Online: 04 August 2010

Elvira Fortunato, Raquel Barros, Pedro Barquinha, Vitor Figueiredo, Sang-Hee Ko Park, Chi-Sun Hwang, and Rodrigo Martins

View Online

Export Citation

ARTICLES YOU MAY BE INTERESTED IN

Sputtering formation of *p*-type SnO thin-film transistors on glass toward oxide complimentary circuits
Applied Physics Letters **97**, 072111 (2010); https://doi.org/10.1063/1.3478213

Microstructure, optical, and electrical properties of *p*-type SnO thin films
Applied Physics Letters **96**, 042113 (2010); https://doi.org/10.1063/1.3277153

Thin-film transistors based on p-type Cu_2O thin films produced at room temperature
Applied Physics Letters **96**, 192102 (2010); https://doi.org/10.1063/1.3428434

Lock-in Amplifiers
... and more, from DC to 600 MHz

AIP Publishing

© 2010 American Institute of Physics.

Transparent p-type SnO_x thin film transistors produced by reactive rf magnetron sputtering followed by low temperature annealing

Elvira Fortunato,[1,a)] Raquel Barros,[1,2] Pedro Barquinha,[1] Vitor Figueiredo,[1] Sang-Hee Ko Park,[3] Chi-Sun Hwang,[3] and Rodrigo Martins[1]

[1]*Departamento de Ciência dos Materiais, CENIMAT/I3N, Faculdade de Ciências e Tecnologia, FCT, CEMOP/UNINOVA, Universidade Nova de Lisboa and, 2829-516 Caparica, Portugal*
[2]*Materiais Avançados, INNOVNANO, SA, 7600-095 Aljustrel, Portugal*
[3]*Electronic and Telecommunications Research Institute, 138 Gajeongro, Yuseong-gu, Daejeon 305-700, Republic of Korea*

(Received 9 February 2010; accepted 7 July 2010; published online 4 August 2010)

P-type thin-film transistors (TFTs) using room temperature sputtered SnO_x ($x<2$) as a transparent oxide semiconductor have been produced. The SnO_x films show p-type conduction presenting a polycrystalline structure composed with a mixture of tetragonal β-Sn and α-SnO_x phases, after annealing at 200 °C. These films exhibit a hole carrier concentration in the range of $\approx 10^{16}-10^{18}$ cm^{-3}; electrical resistivity between 10^1-10^2 Ω cm; Hall mobility around 4.8 cm^2/V s; optical band gap of 2.8 eV; and average transmittance ≈85% (400 to 2000 nm). The bottom gate p-type SnO_x TFTs present a field-effect mobility above 1 cm^2/V s and an ON/OFF modulation ratio of 10^3. © *2010 American Institute of Physics*. [doi:10.1063/1.3469939]

Although the performance achieved with oxide transistors processed at low temperature (T) exceeds far beyond the one obtained with amorphous silicon and organic semiconductors, the oxides reported in the literature are mostly limited to n-type device applications,[1–6] since there is a lack of p-type oxide semiconductors. This confines the field of application of oxide semiconductors solely to unipolar (n-type) devices, inhibiting the fabrication of complementary metal oxide semiconductor (CMOS) based devices.

In spite of the recent p-type oxide thin-film transistors (TFTs) developments, the results achieved so far refer to devices processed at $T>575$ °C limited by a low hole (h) mobility.[7,8] The valence band maxima (VBM) of oxide semiconductors are mainly formed from localized and anisotropic O 2p orbitals, which lead to a low h mobility due to a percolation/hopping conduction.[9] However, if we consider the case of stoichiometric/nonstoichiometric SnO_x, whose structure is associated with the presence of divalent tin, Sn(II), in a layered crystal structure with a Sn–O–Sn sequence and a van der Waals gap between Sn layers, where O atoms are tetrahedrally bonded to Sn ones,[10] this can be changed. In this case the higher-energy region of VBM contains Sn 5s, Sn 5p, and O 2p components nearly equally but very near the VBM the contributions of Sn 5s and O 2p are predominant and can lead to an enhancement in h mobility. This is advantageous in reducing the localization of the valence band edge,[11] since the O 2p component is relatively small and the states near the conduction band minimum are mainly formed by Sn 5p. Under this condition we expect that the hole transport requires structures mainly dominated by α-SnO_x with some embedded β-Sn cations in which VBM is made of pseudoclosed ns^2 orbitals to form hybridized orbitals,[12] as indicated in Fig. 1. The origin of p-type conductivity of SnO_x is mainly attributed to Sn vacancies and O interstitials,[13] that when fully ionized, (respectively, V_{Sn}^{2-} and O_i^{2-}) produce band deformation close to the top of VBM with the formation of acceptor like band states, which for $T>0$ K are partly filled by electrons coming from VBM, according to the quasichemical stoichiometric reactions as follows:[14] $SnO \leftrightarrow Sn^{2+}+2V_{Sn}^{-}+(1/2)O_2$, or $SnO \leftrightarrow Sn^{2+}+V_{Sn}^{2-}+(1/2)O_2$, or $SnO \leftrightarrow Sn^{2+}+V_{Sn}^{-}+O_i^{2-}+(1/2)O_2+V_0^{+}$, giving rise to the formation of two holes (2h), without or with the formation of an oxygen vacancy (V_0^{+}). Here we have to take into account that V_{Sn} form easier than O_i in most densely packed structures. Thus, we expect that the p-type conductivity in α-SnO_x is mainly originated by V_{Sn}, as demonstrated by Togo *et al.*[13] This localized band formation sets the conduction mechanism, as suggested by the SnO layered crystal structure.[8] If there is excess oxygen in the film, some cations will be transformed into Sn^{3+} to maintain charge neutrality. This process can be considered as Sn^{2+} capturing a h and forming weakly bonded holes.

Reports of p-type TFTs are scarce in literature. There are only two recent works employing p-type oxide semiconductors, with Cu_2O (Ref. 7) and SnO.[8] In both works the semiconductor oxide was grown at $T>575$ °C. In this work we report p-type α-SnO_x TFTs deposited by reactive rf sputtering at room temperature followed by annealing at $T=200$ °C. The deposition pressure ($P_{Ar}+P_{O_2}$) and the rf power used were 0.2 Pa and 50 W, respectively. To evaluate the optimal growing conditions for p-type SnO_x films, the oxygen partial pressure ($O_{PP}=P_{O_2}/P_{Ar}+P_{O_2}$) was varied between 0% and 40%. XRD experiments were performed in

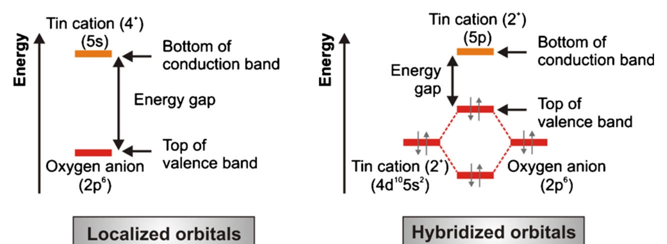

FIG. 1. (Color online) Comparison between the band structure of SnO_2 and SnO. In the case of SnO the top of the valence band consist of hybridized orbital of O 2p and Sn 5s.

[a)]Author to whom correspondence should be addressed. Electronic mail: elvira.fortunato@fct.unl.pt. Tel.: +351 212948562. FAX: +351 212948558.

 © 2010 American Institute of Physics

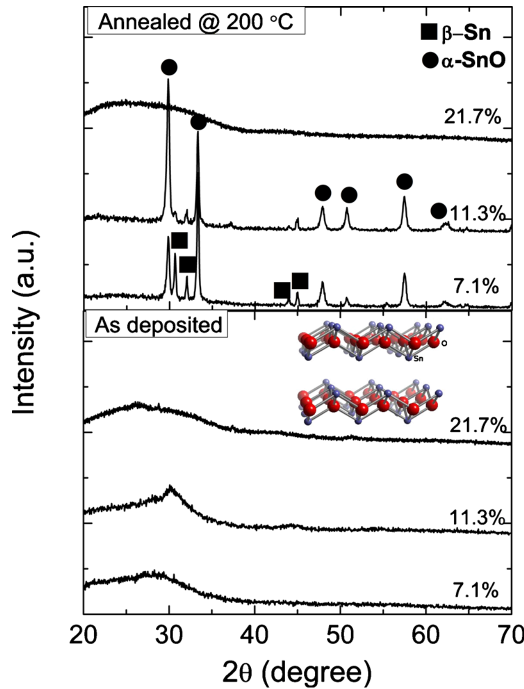

FIG. 2. (Color online) X-ray diffraction patterns for a SnO_x films produced with a O_{PP} between 7.1% and 21.7%, as-deposited and annealed at 200 °C in air atmosphere, with a thickness of 200 nm deposited on a glass substrate. The inset shows the crystal structure of tin (II) oxide (Ref. 18) showing the layered structure of SnO and the wide-stretched open space between the Sn–O–Sn layers.

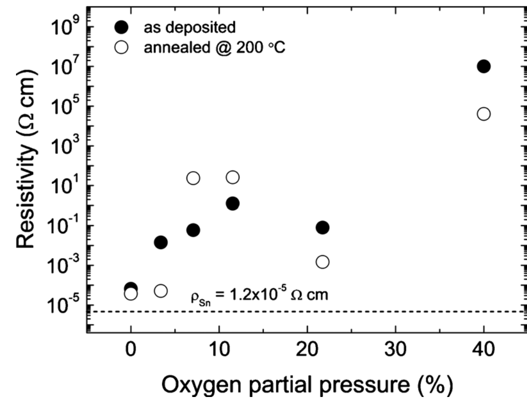

FIG. 3. Dependence of ρ measured by four-point probe on O_{pp}, for as-deposited and annealed SnO_x films. The dashed line represents the electrical resistivity of metallic Sn.

grazing incidence geometry using Cu $K_{\alpha 1,2}$ lines, while optical measurements were performed with a double beam spectrophotometer in the wavelength from 200 to 2500 nm. Electrical transport properties were examined by Hall Effect and conductivity (σ) measurements as a function of T.

Bottom-gate TFTs were fabricated using 30 nm thick α-SnO_x films as semiconductors, while the gate dielectric was a stacked multilayer of Al_2O_3 and TiO_2 (ATO) (Ref. 15) with 220 nm thick deposited on a glass coated with a 200 nm thick indium tin oxide film, acting as gate electrode. For the source-drain electrodes Ti/Au (8/50 nm thick) films were *e*-beam evaporated. The semiconductor and the source-drain electrodes were patterned by lift-off and the TFTs present a width-to-length ratio (W/L) of 1.2, with L=40 μm. The final devices were annealed at 200 °C for 1 h in air and the electrical characterization was performed with an Agilent 4155C semiconductor parameter analyzer and a Cascade Microtech M150 microprobe station.

For $7\% < O_{pp} \leq 11.5\%$ the as-deposited films are amorphous, turning polycrystalline after annealing, as shown in Fig. 2. A mixture of both tetragonal β-Sn and α-SnO phases is observed, being caused by the incomplete Sn oxidation or/and metal segregation due to oxygen disproportionation.[16] SnO generally crystallizes in a tetragonal structure but depending on the conditions of preparation it may also crystallize in an orthorhombic phase.[17,18]

Figure 3 shows the dependence of the electrical resistivity (ρ) on O_{pp} for as-deposited and annealed films. As O_{pp} increases ρ also increases and two different electronic conduction behaviors are observed after annealing, depending on the O_{pp} range. As-deposited α-SnO_x films exhibit n-type conductivity but after annealing at $T=200$ °C the films with $5\% < O_{pp} < 15\%$ present p-type characteristics, as confirmed by Hall effect measurements, where the carrier concentration (N) can be adjusted between $\approx 10^{16}$ and 10^{18} cm^{-3}, corresponding to a maximum Hall mobility (μ_H) of 4.8 cm^2/V s. The p-type characteristics are also confirmed by thermoelectric measurements, where a positive Seebeck coefficient is obtained. This is caused by the fact that for the O_{pp} range mentioned above the p-type conductivity (σ) is controlled by ionized V_{O_i} or V_{Sn} acting as acceptors, while for higher O_{pp} the n-type behavior is due to the existence of Sn atoms in interstitials and V_O.[19–22] For $O_{pp} < 5\%$ a metallic behavior is observed, with $\rho \approx 4.4 \times 10^{-5}$ Ω cm, typical of metallic Sn (1.2×10^{-5} Ω cm). In fact, x-ray data confirm that for $O_{pp} < 5\%$ β-Sn is the predominant phase. As also observed by other authors[8] p-type SnO_x is only obtained at a narrow region of growth conditions, since SnO_2 is formed for higher O_{pp}, whereas metallic Sn precipitates at lower O_{pp}. Since the growth of SnO requires a reducing atmosphere and the vapor pressure of SnO and Sn is high, the deposition at room temperature can be a promising advantage, since inhibits the re-evaporation of deposited thin films.

Figure 4 shows the Arrhenius plots for samples processed with $O_{PP} \cong 7.1\%$ and $O_{PP} \cong 11.5\%$, which do not follow a simple thermally activated transport mechanism. The data could be fitted by a model with two conduction regimes: one at high temperatures ($T \geq 200$ K), controlled by a broad acceptor band located at energy $E_a >$ VBM and partially assisted by phonons ($E_{\omega ph}$) and another one at low temperatures, where the transport is fully governed by phonons as-

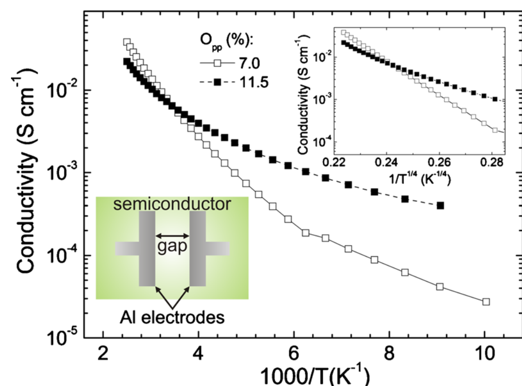

FIG. 4. (Color online) Dependence of σ on T^{-1} for samples fabricated at $O_{PP} \cong 7\%$ and $O_{PP} \cong 11.5\%$. The top right inset shows the σ-$T^{-1/4}$ plot for the same samples. The bottom left inset shows the planar gap cell configuration used for the conductivity measurements.

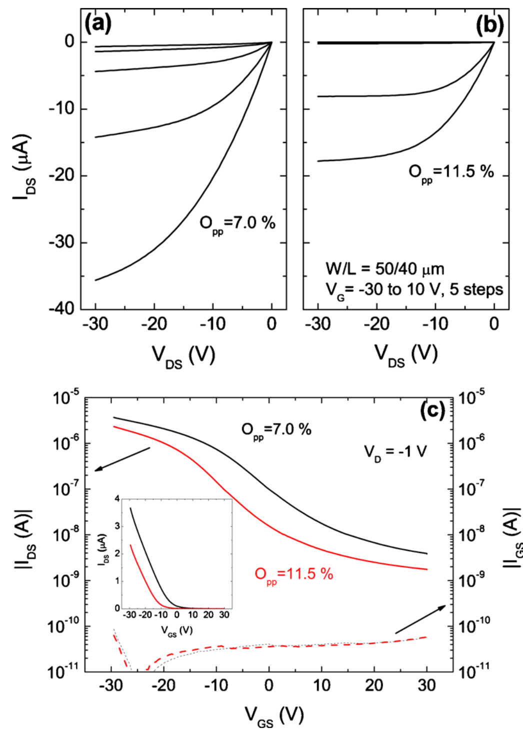

FIG. 5. (Color online) Output characteristics (I_{DS}-V_{DS}) for p-type TFTs working in enhancement mode, where SnO_x is produced with (a) $O_{pp}=7.0$ and (b) $O_{pp}=11.5\%$. (c) Transfer characteristics ($|I_{DS}$-$V_{GS}|$), left axis and leakage current ($|I_{GS}$-$V_{GS}|$), right axis, for SnO_x TFTs annealed in air at 200 °C, where SnO_x is produced with $O_{pp}=7.0$ and 11.5%. The inset shows the $|I_{DS}$-$V_{GS}|$ plots represented in linear scale, for V_T extraction.

sisting the conduction mechanism,[23] translated by the following formula:

$$\sigma \cong \sigma_0 e^{(E_a+E_{\omega ph})/k_B T} + \sigma_{0H} e^{(E_{\omega ph}/k_B T)} \quad (1)$$

where σ_0 and σ_{0H} are the pre-exponential factors of the two conduction pathways referred above and k_B is the Boltzmann constant. Under this condition we estimate $E_a \cong 0.10-0.90$ eV while $E_{\omega ph} \cong 0.05-0.03$ eV, which agrees with the Mott model[23] where there exists a localized disorder. However, better straight lines are obtained in the log σ versus $T^{-1/4}$ plot (inset in Fig. 4), presumably not related to variable-range hopping but rather to percolation conduction. In this case, the random distribution of Sn^{2+} ions modulates the electronic structure around the valence band edge and may form statistical potential barrier distribution with 0.10 eV high and a few tens of meV width, agreeing with the values predicted by Kamiya *et al.*[9]

Figures 5(a) and 5(b) show the output characteristics of two α-SnO_x TFTs produced with $O_{pp}=7.0$ and 11.5%, after annealing in air at 200 °C. The devices show different behaviors, as expected, with clear linear and saturation regions and do not present significant current crowding for low V_{DS}, indicating low series resistance in source-drain contacts with SnO_x. Figure 5(c) shows the transfer characteristics with $V_{DS}=-1$ V for the same devices. The right axis shows the leakage current (I_{GS}) and the obtained value is quite low (<0.1 nA) for the V_{GS} range used, showing that ATO provides good insulating properties even for large negative bias. The ON/OFF ratio of both devices is 10^3, the field-effect mobility (μ_{FE}, calculated by the transconductance in the linear regime) is between 1.1 and 1.2 cm^2/V s, while the V_T was varying between −5 and −12 V, for an O_{pp} of 7.0% and 11.5%, respectively, mainly due to the increase in interface states between the gate insulator and the semiconductor. Here $\mu_{FE} < \mu_H$, which is explained by hole traps at the insulator interface or by defects in the band gap near VBM.

We have demonstrated the possibility to produce transparent p-type α-SnO_x semiconductors by reactive magnetron sputtering without intentional substrate heating, after a low T annealing at 200 °C. The α-SnO_x films are polycrystalline presenting a mixture of both tetragonal β-Sn and α-SnO phases. The p-type conductivity is obtained for a narrow O_{pp} range, (5%–15%), where these films exhibit 10^{16} $cm^{-3} < N < 10^{18}$ cm^{-3}, 10^1 Ω cm $< \rho < 10^2$ Ω cm, reaching a maximum of $\mu_H \approx 4.8$ cm^2/V s. The bottom gate p-type α-SnO_x TFTs with channel layer thickness of 30 nm are 85% transparent in the visible range of the electromagnetic spectrum, presenting $\mu_{FE} \approx 1.1-1.2$ cm^2/V s and an ON/OFF ratio of 10^3.

This work was funded by FCT-MCTES through Project Nos. PTDC/CTM/73943/2006 and PTDC/EEA-ELC/64975/2006, ERC 2008 Advanced Grant (INVISIBLE No. 228144), and IT R&D program of MKE (No. 2006-S079-03) from ETRI Korea. We thank K. Nomura for the Seebeck measurements, N. Franco and N. Neves for the XRD.

[1]E. M. C. Fortunato, P. M. C. Barquinha, A. Pimentel, A. M. F. Goncalves, A. J. S. Marques, L. M. N. Pereira, and R. F. P. Martins, Adv. Mater. (Weinheim, Ger.) **17**, 590 (2005).
[2]E. Fortunato, P. Barquinha, A. Pimentel, L. Pereira, G. Goncalves, and R. Martins, Phys. Status Solidi (RRL) **1**, R34 (2007).
[3]P. Barquinha, L. Pereira, G. Goncalves, R. Martins, and E. Fortunato, J. Electrochem. Soc. **156**, H161 (2009).
[4]E. M. C. Fortunato, L. M. N. Pereira, P. M. C. Barquinha, A. M. B. do Rego, G. Goncalves, A. Vila, J. R. Morante, and R. F. P. Martins, Appl. Phys. Lett. **92**, 222103 (2008).
[5]G. Gonçalves, P. Barquinha, L. Pereira, N. Franco, E. Alves, R. Martins, and E. Fortunato, Electrochem. Solid-State Lett. **13**, H20 (2010).
[6]E. Fortunato, L. Pereira, P. Barquinha, I. Ferreira, R. Prabakaran, G. Goncalves, A. Goncalves, and R. Martins, Philos. Mag. **89**, 2741 (2009).
[7]K. Matsuzaki, K. Nomura, H. Yanagi, T. Kamiya, M. Hirano, and H. Hosono, Appl. Phys. Lett. **93**, 202107 (2008).
[8]Y. Ogo, H. Hiramatsu, K. Nomura, H. Yanagi, T. Kamiya, M. Hirano, and H. Hosono, Appl. Phys. Lett. **93**, 032113 (2008).
[9]T. Kamiya and H. Hosono, NPG Asia Mater **2**, 15 (2010).
[10]I. Lefebvre, M. A. Szymanski, J. Olivier-Fourcade, and J. C. Jumas, Phys. Rev. B **58**, 1896 (1998).
[11]H. Yanagi, H. Kawazoe, A. Kudo, M. Yasukawa, and H. Hosono, J. Electroceram. **4**, 407 (2000).
[12]Y. Ogo, H. Hiramatsu, K. Nomura, H. Yanagi, T. Kamiya, M. Kimura, M. Hirano, and H. Hosono, Phys. Status Solidi A **206**, 2187 (2009).
[13]A. Togo, F. Oba, I. Tanaka, and K. Tatsumi, Phys. Rev. B **74**, 195128 (2006).
[14]Z. M. Jarzebski, *Oxide Semiconductors* (Pergamon, Oxford, 1973).
[15]ITO/ATO-coated glass substrates from Planar Systems, I. E., Finland (2004).
[16]J. Geurts, S. Rau, W. Richter, and F. J. Schmitte, Thin Solid Films **121**, 217 (1984).
[17]W. K. Choi, H. Sung, K. H. Kim, J. S. Cho, S. C. Choi, H. J. Jung, S. K. Koh, C. M. Lee, and K. Jeong, J. Mater. Sci. Lett. **16**, 1551 (1997).
[18]Properties of tin monoxide from www.webelements.com.
[19]E. Leja, J. Korecki, K. Krop, and K. Toll, Thin Solid Films **59**, 147 (1979).
[20]E. Leja, T. Pisarkiewicz, and A. Kolodziej, Thin Solid Films **67**, 45 (1980).
[21]T. M. Uen, K. F. Huang, M. S. Chen, and Y. S. Gou, Thin Solid Films **158**, 69 (1988).
[22]K. F. Huang, T. M. Uen, Y. S. Gou, C. R. Huang, and H. C. Yang, Thin Solid Films **148**, 7 (1987).
[23]N. F. Mott and E. A. Davis, *Electronic Processes in Non-Crystalline Materials*, 2nd ed. (Clarendon, Oxford, 1979).